T matrices and current correlation functions for a relativistic quark model with confinement

L. S. Celenza, Bo Huang, and C. M. Shakin*
Department of Physics and Center for Nuclear Theory, Brooklyn College of the City University of New York, Brooklyn, New York 11210
(Received 10 September 1998)

We describe some properties of a relativistic model of confinement and show how that model may be used to construct *T* matrices for quark-antiquark systems. [In the absence of the confinement model, our Lagrangian reduces to that of the SU(3)-flavor Nambu–Jona-Lasinio model.] If we have absolute confinement, our *T* matrix is expressed in terms of bound states (or resonances), without the presence of quark scattering states. We find that is a straightforward matter to describe singlet-octet and pseudoscalar-axial-vector mixing in this formalism. We also demonstrate that the construction of the *T* matrices of the model allows us to obtain expressions for various current correlation functions, once the meson decay constants are calculated. That calculation is readily made starting with knowledge of the *T* matrix. The most complex situation we consider is that of the η-η' system, with both singlet-octet and pseudoscalar-axial-vector mixing, calculated in the presence of a (covariant) confinement model. Values of masses, coupling constants and mixing angles are given for the π, ω, ϕ, η, and η' mesons and for some of their radial excitations. [S0556-2813(99)02102-0]

PACS number(s): 12.39.Ki, 12.38.Aw, 14.40.Aq, 24.85.+p

I. INTRODUCTION

In this work we are interested in obtaining information concerning meson structure using a relativistic quark model that includes a description of (Lorentz vector) confinement. In the absence of the confinement model, our Lagrangian reduces to that of the SU(3)-flavor Nambu–Jona-Lasinio (NJL) model [1]. The Lagrangian we use exhibits chiral symmetry in the absence of a quark mass matrix:

$$\mathcal{L}=\bar{q}(i\not\partial-m^0)q+\frac{G_S}{4}\sum_{i=0}^{8}[(\bar{q}\lambda^i q)^2+(\bar{q}i\gamma_5\lambda^i q)^2]$$
$$+\frac{G_D}{2}\{\det[\bar{q}(1+\gamma_5)q]+\det[\bar{q}(1-\gamma_5)q]\}$$
$$-\frac{G_V}{4}\sum_{i=0}^{8}[(\bar{q}\gamma^\mu\lambda^i q)^2+(\bar{q}\gamma^\mu\gamma_5\lambda^i q)^2]+\mathcal{L}_{\rm conf}. \tag{1.1}$$

We have $m^0=\mathrm{diag}(m_u^0,m_d^0,m_s^0)$ as the current quark mass matrix. The term proportional to G_D is the 't Hooft interaction. The λ_i $(i=1,\ldots,8)$ are the Gell-Mann matrices and $\lambda_0=\sqrt{2/3}I$, where I is the unit matrix in flavor space.

Since our confinement model has been described in detail elsewhere [2–6], we only provide a schematic description in this work. In the generalized model, we introduce confinement by calculating a vertex function for the confining interaction V^C. For example, for the study of vector mesons, the vertex is denoted as $\Gamma^\mu(P,k)$ (see Fig. 1). The vertex satisfies the inhomogeneous equation shown in Fig. 1, where it is represented by the shaded triangular area. As may be seen in the second part of the figure, the vertex serves to sum a ''ladder'' of confining interactions. We find that the vertex is singular at those energies for which the homogeneous equation has a solution. These singularities are at the energies of the bound states in the confining field. Another important property of the vertex is that it is equal to zero when $|\vec{k}|=k_{on}$, with $k_{on}=[P^2/4-m^2]^{1/2}$, if $\vec{P}=0$. That is the point where the quark and antiquark would go on their (positive) mass shells [6].

In the study of the NJL model one needs to calculate vacuum-polarization functions $J(P^2)$, such as those depicted in Fig. 2(a). To introduce confinement, we sum a series of confining interactions, as in Fig. 2(b). The inclusion of the vertex function (shaded triangular region) in the calculation of $J(P^2)$, as shown in Fig. 2, serves to define the vacuum-polarization function for the theory with confinement. That function does not have the cut starting at $P^2=(2m_q)^2$, that would be present in the absence of a model of confinement.

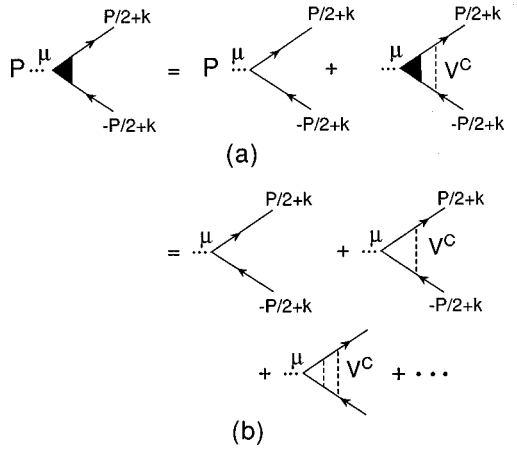

FIG. 1. (a) The equation for the vertex operator $\Gamma^\mu(P,k)$ is shown. The vertex is represented by the filled triangular area and the dashed line represents the confining interaction (see Fig. 2). (b) A perturbation expansion is shown for the equation in (a). We see that the vertex sums a ''ladder'' of confining interactions.

*Electronic address: CASBC@CUNYVM.CUNY.EDU

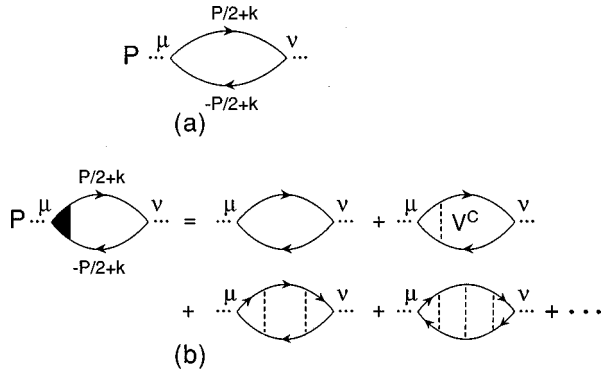

FIG. 2. (a) The diagram shows the basic vacuum-polarization diagram of the NJL model that is evaluated in the calculation of the tensor $J^{\mu\nu}(P^2)$. (b) The diagram serves to define the tensor $J^{\mu\nu}(P^2)$ when confinement effects are included. The shaded triangular area represents the confining vertex of Fig. 1. The right-hand side of the figure shows a perturbative expansion for $J^{\mu\nu}(P^2)$.

Thus, $J(P^2)$ is a real function with singularities reflecting those of the vertex function.

In Sec. II we describe various aspects of our relativistic confinement model and give some equations for the vertex function for pseudoscalar excitations. In Sec. III we discuss radial excitations of the pion and present the form taken by the quark T matrix in this case. In Sec. IV we extend the considerations of Sec. III to the case of $\pi - a_1$ mixing. In Sec. V we describe the T matrix that exhibits resonances describing the ω and ϕ mesons and some of their radial excitations. In Sec. VI we take up the topic of singlet-octet mixing for the η and η' mesons, while in Sec. VII we extend that analysis to include pseudoscalar-axial-vector mixing. Finally, Sec. VIII contains some further discussion and conclusions.

II. RELATIVISTIC CONFINEMENT MODEL

To construct a momentum-space confinement model, we start with the form $V^C = \kappa_V r \exp[-\mu r]$. Here μ is a small parameter introduced to soften the momentum-space singularities of the Fourier transform of $V^C(r)$:

$$V^C(\vec{k}-\vec{k}') = -8\pi\kappa\left[\frac{1}{[(\vec{k}-\vec{k}')^2+\mu^2]^2} - \frac{4\mu^2}{[(\vec{k}-\vec{k}')^2+\mu^2]^3}\right]. \tag{2.1}$$

As μ is reduced in value, the potential approximates a linear potential to a greater degree. We use $\mu = 0.020\,\mathrm{GeV}$ in our calculations of the properties of light mesons. That leads to a maximum value $V^C_{\max} = \kappa_V/(\mu e) = 1.06\,\mathrm{GeV}$, when $\kappa_V = 0.0575\,\mathrm{GeV}^2$ and $\mu = 0.020\,\mathrm{GeV}$. (We note that relativistic factors in our equations put the *effective* value of $V^C_{\max}$ at about 1.7 GeV.) We use Lorentz-vector confinement, so that our potential is $\gamma^\mu(1) V^C(\vec{k}-\vec{k}')\gamma_\mu(2)$ in momentum space. We have seen, in a study of vector mesons, that if we use Lorentz-scalar confinement rather than Lorentz-vector confinement, we need to take $\kappa_S \simeq 2\kappa_V$ to obtain essentially the same spectrum of states. Therefore, $\kappa_S = 0.12\,\mathrm{GeV}^2$. It is the latter value that can profitably be compared to the value used for the string tension for massive quark systems, $\kappa_{NR} \sim 0.18\,\mathrm{GeV}^2$, for the case of Lorentz-scalar confinement. These comments suggest that, while we quote $\kappa_V = 0.0575\,\mathrm{GeV}^2$ as our value of κ_V for light mesons, the corresponding κ_{NR} is about two-thirds of the string tension in massive quark systems.

To illustrate the relativistic effects that lead to an enhanced value of $V^C_{\max}$, we may consider an equation for a (confining) vertex function for pseudoscalar mesons. In this case, we write the vertex associated with a ladder sum of confining interactions as $\overline{\Gamma}_5(P,k) = \gamma_5 \Gamma_5(P,k)$. It is found useful to introduce matrix elements of $\overline{\Gamma}_5(P,k)$

$$\Lambda^{(+)}(\vec{k})\overline{\Gamma}_5(P,k)\Lambda^{(-)}(-\vec{k}) = \Gamma_5^{+-}(P,k)\Lambda^{(+)}(\vec{k})\gamma_5\Lambda^{(-)}(-\vec{k}) \tag{2.2}$$

and

$$\Lambda^{(-)}(-\vec{k})\overline{\Gamma}_5(P,k)\Lambda^{(+)}(\vec{k}) = \Gamma_5^{-+}(P,k)\Lambda^{(-)}(-\vec{k})\gamma_5\Lambda^{(+)}(\vec{k}), \tag{2.3}$$

where

$$\Lambda^{(+)}(\vec{k}) = \frac{\not{k}+m}{2m}, \tag{2.4}$$

$$\Lambda^{(-)}(-\vec{k}) = \frac{\not{\tilde{k}}+m}{2m}, \tag{2.5}$$

with $k^\mu = [E(\vec{k}),\vec{k}]$ and $\tilde{k}^\mu = [-E(\vec{k}),\vec{k}]$. The functions $\Gamma_5^{+-}(P,k)$ and $\Gamma_5^{-+}(P,k)$ are defined in the rest frame of the meson ($\vec{P}=0$). They appear naturally when calculating vacuum-polarization integrals in our relativistic quark model.

The function $\Gamma_5^{+-}(P^0,|\vec{k}|)$ satisfies the equation

$$\Gamma_5^{+-}(P^0,|\vec{k}|) = 1 + \int \frac{d^3k'}{(2\pi)^3}\frac{V^C(\vec{k}-\vec{k}')}{P^0-2E(\vec{k}')} \times\left[\frac{2E(\vec{k})E(\vec{k}')-m^2}{E(\vec{k})E(\vec{k}')}\right]\Gamma_5^{+-}(P^0,|\vec{k}'|), \tag{2.6}$$

for Lorentz-vector confinement. Here $E(\vec{k}) = [\vec{k}^2+m^2]^{1/2}$.

It is helpful to introduce the wave function

$$\Psi_5(P^0,|\vec{k}|) = \frac{\Gamma_5^{+-}(P^0,|\vec{k}|)}{P^0-2E(\vec{k})}, \tag{2.7}$$

which satisfies the equation

$$[P^0-2E(\vec{k})]\Psi_5(P^0,|\vec{k}|)=1+\int\frac{d^3k'}{(2\pi)^3}V^C(\vec{k}-\vec{k}')\times\left[\frac{2E(\vec{k})E(\vec{k}')-m^2}{E(\vec{k})E(\vec{k}')}\right]\Psi_5(P^0,|\vec{k}'|). \tag{2.8}$$

We may also introduce the solutions of the homogeneous equation

$$[E_n-2E(\vec{k})]\Psi_5(E_n,|\vec{k}|)=\int\frac{d^3k'}{(2\pi)^3}V^C(\vec{k}-\vec{k}')\times\left[\frac{2E(\vec{k})E(\vec{k}')-m^2}{E(\vec{k})E(\vec{k}')}\right]\Psi_5(E_n,|\vec{k}'|). \tag{2.9}$$

The energies E_n form a discrete set, if the potential is absolutely confining. In that case, we need not supplement the denominator in Eq. (2.7) with an $i\epsilon$ factor. [This feature may be traced to the infrared behavior of the confining potential $V^C(\vec{k}-\vec{k}')$.]

Note that if the quark mass is very large, we can replace the bracketed quantity in Eq. (2.9) by unity. Equation (2.9) then represents a momentum-space version of an equation for bound states in confining potential $V^C(r)=\kappa r\exp[-\mu r]$. We may define a vertex function for a bound state

$$\Gamma_5^{+-}(E_n,|\vec{k}|)=[E_n-2E(\vec{k})]\Psi_5(E_n,|\vec{k}|). \tag{2.10}$$

There is a zero in the vertex function when $|\vec{k}|=k_{on}$ when $E_n=2E(k_{on})$. When making calculations in momentum space, it is that zero of the vertex function that eliminates any long-range (scattering) component of the wave function.

We may return to the inhomogeneous equation [Eq. (2.8)] and note that for large $|\vec{k}|$, such that $2E(\vec{k})\gg P^0$,

$$\Psi_5(P^0,|\vec{k}|)\simeq-\frac{1}{2|\vec{k}|}, \tag{2.11}$$

since $\Gamma_5^{+-}(P^0,|\vec{k}|)\to 1$ for large $|\vec{k}|$. Once we solve the inhomogeneous equation for $\Psi_5(P^0,|\vec{k}|)$, we obtain $\Gamma_5^{+-}(P^0,|\vec{k}|)$ from Eq. (2.7). The factor $P^0-2E(\vec{k})$ induces a zero in $\Gamma_5^{+-}(P^0,|\vec{k}|)$ at $|\vec{k}|=k_{on}$, if P^0 is large enough for the equation

$$k_{on}=[(P^0/2)^2-m_q^2]^{1/2} \tag{2.12}$$

to have a solution for k_{on} real. That feature may be seen in Fig. 3, where we show $\Gamma_5^{+-}(P^0,|\vec{k}|)$ for several values of P^0.

The equation for $\Gamma_5^{-+}(P^0,|\vec{k}|)$ is

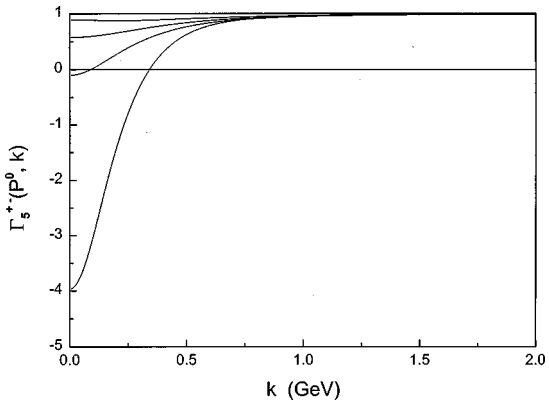

FIG. 3. The figure shows the values of $\Gamma_5^{+-}(P^0,|\vec{k}|)$ for various P^0. Starting with uppermost curve we have $P^0=0.0$ GeV, $P^0=0.5$ GeV, $P^0=0.75$ GeV, $P^0=1.0$ GeV. Note that $\Gamma_5^{+-}(P^0,k_{on})=0$, where $k_{on}=[(P^0/2)^2-m_q^2]^{1/2}$. Here $m_q=0.364$ GeV and $\kappa=0.0575$ GeV^2.

$$\Gamma_5^{-+}(P^0,|\vec{k}|)=1-\int\frac{d^3k'}{(2\pi)^3}\frac{V^C(\vec{k}-\vec{k}')}{P^0+2E(\vec{k}')}\times\left[\frac{2E(\vec{k})E(\vec{k}')-m^2}{E(\vec{k})E(\vec{k}')}\right]\Gamma_5^{-+}(P^0,|\vec{k}'|). \tag{2.13}$$

It is worth noting that if we were to use Lorentz-scalar confinement, we would have

$$\Gamma_{5,\,\mathrm{scal}}^{+-}(P^0,|\vec{k}|)=1+\int\frac{d^3k'}{(2\pi)^3}\frac{V^C(\vec{k}-\vec{k}')}{P^0-2E(\vec{k}')}\times\frac{E(\vec{k})E(\vec{k}')+m^2-\vec{k}\cdot\vec{k}'}{2E(\vec{k})E(\vec{k}')}\Gamma_{5,\,\mathrm{scal}}^{+-}(P^0,|\vec{k}'|). \tag{2.14}$$

We see that as m is made large, $\Gamma_5^{+-}(P^0,|\vec{k}|)$ and $\Gamma_{5,\,\mathrm{scal}}^{+-}(P^0,|\vec{k}|)$ satisfy the same simple equation

$$\Gamma_5^{+-}(P^0,|\vec{k}|)=1+\int\frac{d^3k'}{(2\pi)^3}V^C(\vec{k}-\vec{k}')\frac{\Gamma_5^{+-}(P^0,|\vec{k}'|)}{P^0-2E(\vec{k}')}. \tag{2.15}$$

Thus, the value of κ for Lorentz-scalar or Lorentz-vector confinement would be the same, when studying pseudoscalar mesons of large mass.

For the sake of completeness, we present the equation for $\Gamma_{5,\,\mathrm{scal}}^{-+}(P^0,|\vec{k}|)$:

$$\Gamma_{5,\,\mathrm{scal}}^{-+}(P^0,|\vec{k}|)=1-\int\frac{d^3k'}{(2\pi)^3}\frac{V^C(\vec{k}-\vec{k}')}{P^0+2E(\vec{k}')}\times\frac{E(\vec{k})E(\vec{k}')+m^2-\vec{k}\cdot\vec{k}'}{2E(\vec{k})E(\vec{k}')}\Gamma_{5,\,\mathrm{scal}}^{-+}(P^0,|\vec{k}'|). \tag{2.16}$$

For large m, Eqs. (2.13) and (2.16) take on the same form

$$\Gamma_5^{-+}(P^0,|\vec{k}|)=1-\int\frac{d^3k'}{(2\pi)^3}V^C(\vec{k}-\vec{k}')\frac{\Gamma_5^{-+}(P^0,|\vec{k}'|)}{P^0+2E(\vec{k}')}. \tag{2.17}$$

As a final point, we note that when we study the upsilon system of states, we use $\kappa=0.176\,\mathrm{GeV}^2$ in our model, which is quite consistent with general expectations concerning the value of the string tension for a nonrelativistic system, as noted above.

It is possible to make our relativistic confinement model covariant [3]. That is done by introducing the vectors

$$k_c^\mu=k^\mu-\frac{(k\cdot P)P^\mu}{P^2} \tag{2.18}$$

and

$$k_c'^\mu=k'^\mu-\frac{(k'\cdot P)P^\mu}{P^2}, \tag{2.19}$$

and replacing Eq. (2.1) by

$$V^C(k_c-k_c')=-8\pi\kappa\left[\frac{1}{[(k_c-k_c')^2-\mu^2]^2}+\frac{4\mu^2}{[(k_c-k_c')^2-\mu^2]^3}\right]. \tag{2.20}$$

Since, in the meson rest frame ($\vec{P}=0$), $k_c^\mu=(0,\vec{k})$, and $k_c'^\mu=(0,\vec{k}')$, V^C of Eq. (2.20) reduces to V^C of Eq. (2.1). We may use the covariant nature of the model to construct covariant vertex functions for the confining interaction. That feature of the model will be discussed in Sec. III.

There are some similarities of our model to the global color model [7–9]. There, in some applications, the gluon propagator is written as

$$G_{\mu\nu}(k)=-\tilde{g}_{\mu\nu}(k)G(k^2) \tag{2.21}$$

in the Landau gauge, with $\tilde{g}_{\mu\nu}(k)=g_{\mu\nu}-k_\mu k_\nu/k^2$ [10,11]. Further, $G(k^2)=G_{\mathrm{UV}}(k^2)+G_{\mathrm{IR}}(k^2)$. The low-$k^2$ behavior is given by

$$G_{\mathrm{IR}}=\frac{16\pi^2}{3}ak^2e^{-\mu k^2} \tag{2.22}$$

in Euclidean momentum space. In Ref. [11], it is remarked that this form of $G_{\mathrm{IR}}(k^2)$ provides what is effectively a linear potential for $r<1.0$ fm. [The form of Eq. (2.22) is chosen to avoid the singular nature of Eq. (2.1) at small μ, for example.] Since we use Lorentz-vector confinement, our potential $\gamma^\mu(1)V^C(\vec{k}-\vec{k}')\gamma_\mu(2)$, plays a role similar to that played by $G_{\mathrm{IR}}(k^2)$ in implementing confinement, since the gluons are vector fields. However, our calculations are made in Minkowski momentum space, while those global color model are made in Euclidean momentum space and an analytic continuation is required to obtain meson masses and other properties [10,11].

III. RADIAL EXCITATIONS OF THE PION

For the moment, we will neglect π-a_1 mixing and return to that aspect of the problem in Sec. V. In this case we have a T matrix of the form

$$T_\pi(P^2)=i\gamma_5T^{PP}(P^2)i\gamma_5, \tag{3.1}$$

with

$$T^{PP}(P^2)=-\frac{G_S}{1-G_SJ^{PP}(P^2)}. \tag{3.2}$$

(We suppress reference to isospin in these expressions.) We define the function

$$-iJ^{PP}(P^2)=-n_cn_f\mathrm{Tr}\int\frac{d^4k}{(2\pi)^4}\times[iS(P/2+k)i\gamma_5iS(-P/2+k)i\gamma_5], \tag{3.3}$$

in the absence of confinement. If we introduce a confinement vertex $\overline{\Gamma}_5(P,k)$, we define

$$-iJ^{PP}(P^2)=-n_cn_f\mathrm{Tr}\int\frac{d^4k}{(2\pi)^4}\times[S(P/2+k)\overline{\Gamma}_5(P,k)S(-P/2+k)\gamma_5]. \tag{3.4}$$

In general, we would have

$$\Gamma_5(P,k)=b_0(P,k)+\not{P}b_1(P,k)+\not{k}b_2(P,k)+i\sigma^{\mu\nu}P_\mu k_\nu b_3(P,k). \tag{3.5}$$

However, for our model of Lorentz-vector confinement, in which there is no energy transfer in the frame with $\vec{P}=0$, we find that we need only two terms:

$$\Gamma_5(P,k)=b_0(\sqrt{P^2},\sqrt{-k_c^2})+\not{P}b_1(\sqrt{P^2},\sqrt{-k_c^2}). \tag{3.6}$$

Recall that k_c was defined in Eq. (2.18). Note that in the frame where $\vec{P}=0$, Eq. (3.6) may be written as

$$\Gamma_5(P^0,|\vec{k}|)=b_0(P^0,|\vec{k}|)+\gamma_0P^0b_1(P^0,|\vec{k}|). \tag{3.7}$$

We may obtain the scalar invariants appearing in Eq. (3.6) by identifying Eqs. (3.6) and (3.7) in the meson rest frame.

Using the definition of $\overline{\Gamma}_5(P,k)$, we have the following relations between b_0, b_1, Γ^{+-}, and Γ^{-+}:

$$\Gamma_5^{+-}(P^0,|\vec{k}|)=b_0(P^0,|\vec{k}|)-\frac{P^0m}{E(k)}b_1(P^0,|\vec{k}|) \tag{3.8}$$

and

$$\Gamma_5^{-+}(P^0,|\vec{k}|)=b_0(P^0,|\vec{k}|)+\frac{P^0m}{E(k)}b_1(P^0,|\vec{k}|). \tag{3.9}$$

Also, when the quarks go on mass shell, $P^0=2E(k)$, so that

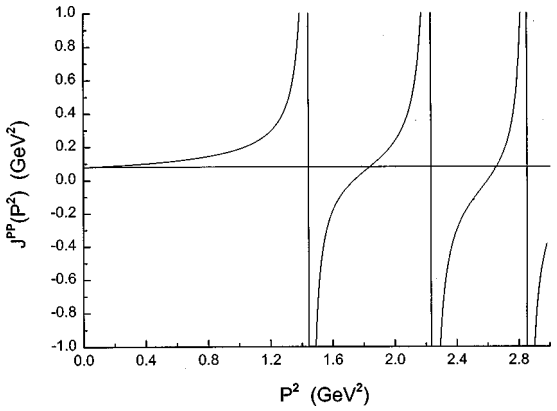

FIG. 4. Values of $J^{PP}(P^2)$ are shown. The horizontal line represents $G_S^{-1}=0.08134\,\mathrm{GeV}^2$. The intersection of that line with $J^{PP}(P^2)$ provides the solution of Eq. (3.13). The mass values are those for the $\pi(1S)$, $\pi(2S)$, and $\pi(3S)$ states in the absence of π-a_1 coupling.

$$\Gamma_5^{+-}(P^0,k_{on})=b_0(P^0,k_{on})-2mb_1(P^0,k_{on}), \quad (3.10)$$

$$=0, \quad (3.11)$$

which is a characteristic of our model of confinement (see Fig. 3). It is this feature that serves to eliminate the (unphysical) $q\bar{q}$ cut from the vacuum-polarization functions.

Now we consider the solution of

$$1-G_S J^{PP}(P^2)=0 \quad (3.12)$$

to obtain the mass values of the pion and its radially excited states. It is instructive to present a graphical solution of Eq. (3.12), which we rewrite in the form

$$G_S^{-1}-J^{PP}(P^2)=0. \quad (3.13)$$

In Fig. 4 we show $J^{PP}(P^2)$ calculated for Lorentz-vector confinement, with $\kappa=0.0575\,\mathrm{GeV}^2$ and $m_q=0.364\,\mathrm{GeV}$. It is seen from the figure that $J^{PP}(P^2)$ has singularities (indicated by the vertical lines). These appear at the values of P^2 where the homogeneous equation, Eq. (2.9), has solutions. These are the energies of the bound states in the confining field. The states are moved to lower energy when the attractive NJL interaction is included via the solution of Eq. (3.13). In Fig. 4 we have shown $G_S^{-1}=0.08134\,\mathrm{GeV}^2$ as a horizontal line. The points where the horizontal line intersects $J^{PP}(P^2)$ determine the energies of the $\pi(1S)$, $\pi(2S)$, and $\pi(3S)$ states.

TABLE I. Values of the mixing angle for the pion and its radial excitations (see Table II).

Energy (GeV)	Channel	θ (rad)	θ (deg)
0.138	T_1	-0.059	$-3.39°$
1.18	T_1	2.20	126°
1.36	T_2	-1.52	$-87.8°$
1.47	T_2	0.55	31.8°
1.63	T_1	0.047	2.68°
1.68	T_1	2.06	118°

TABLE II. Values of the mixing angle for the pion and its radial excitations when all resonances are expressed in the form used for T_1 given in Eq. (4.9) (see Fig. 5).

Energy (GeV)	θ (deg)	Nature of state
0.138	$-3.39°$	pionlike--$\pi(1S)$
1.18	126°	mixed state
1.36	2.20°	pionlike--$\pi(2S)$
1.47	122°	mixed state
1.63	2.68°	pionlike--$\pi(3S)$
1.68	118°	mixed state

The corresponding calculation is more complicated if pseudoscalar-axial-vector coupling is included for the pion. In that case we deal with a T matrix of dimension 2, as described in some detail in Sec. IV. We find six states in the region $P^2\leqslant 3\,\mathrm{GeV}^2$ (see Tables I and II and Fig. 5).

In the absence of π-a_1 mixing, we may write

$$\frac{G_S}{1-G_S J^{PP}(P^2)}\simeq-\frac{g^2_{\pi' qq}}{P^2-m^2_{\pi'}} \quad (3.14)$$

with

$$\frac{1}{g^2_{\pi' qq}}=\left.\frac{\partial J^{PP}(P^2)}{\partial P^2}\right|_{P^2=m^2_{\pi'}} \quad (3.15)$$

near a bound state or resonance. As a final step, we include the confinement vertex for the external lines and write

$$T_\pi(P,k',k)\simeq[b_0(P,k')+\not{P}b_1(P,k')]\times\frac{i\gamma_5 g^2_{\pi' qq}}{P^2-m^2_\pi}i\gamma_5[b_0(P,k)+\not{P}b_1(P,k)] \quad (3.16)$$

(see Fig. 6).

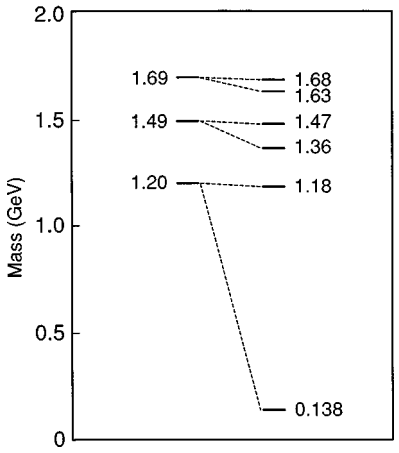

FIG. 5. On the left-hand side of the figure are the doublets found in the confining field. When the NJL interaction is included, the spectrum on the right side is obtained (see Table I). The states at $P^0=0.138\,\mathrm{GeV}$, $P^0=1.36\,\mathrm{GeV}$, and $P^0=1.63\,\mathrm{GeV}$ are the $\pi(1S)$, $\pi(2S)$, and $\pi(3S)$ states with small mixing angles (see Table II.)

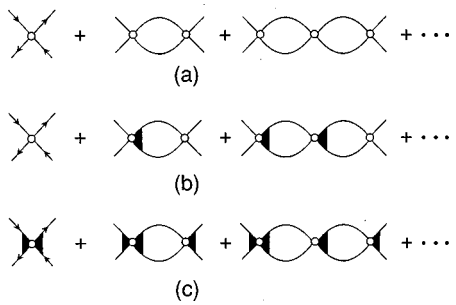

FIG. 6. (a) A Born term and a series of vacuum-polarization diagrams for the NJL model without confinement is shown. (b) The vacuum-polarization diagrams of (a) are modified by inclusion of the vertex of the confining interaction. (c) The vertex for the confining interaction is added for the external lines, defining T matrices of the form $T(P,k',k)$ (see Fig. 7).

It is useful to include the propagators associated with the external lines. We define

$$G_\pi(P,k',k)=[S(-P/2+k')\overline{\Gamma}_5(P,k')i\gamma_5 S(P/2+k')] \times\frac{g^2_{\pi' qq}}{P^2-m^2_{\pi'}} \times[S(P/2+k)i\gamma_5\overline{\Gamma}_5(P,k)S(-P/2+k)], \tag{3.17}$$

where we have again suppressed reference to isospin in the vertex functions for simplicity.

The manipulations of this section may be understood with reference to Fig. 6. In Fig. 6(a) we show the diagrams that are summed in the absence of confinement to yield a T matrix. In Fig. 6(b), we include confinement in the calculation of the vacuum-polarization functions, $J(P^2)$. Finally, we introduce the confinement vertex functions associated with the external lines. Therefore, Fig. 6(c) is in correspondence with $T_\pi(P,k',k)$ of Eq. (3.16). This correspondence is more clearly seen in Fig. 7(a), where we have introduced the propagator for the pion or one of its radially excited states. (As remarked earlier, it is best to neglect confinement for the $\pi(138)$, since the properties of that meson are extremely sensitive to small violations of chiral symmetry.) If we introduce the propagators for the external lines, Fig. 7(a) is in correspondence with $G_\pi(P,k',k)$ of Eq. (3.17).

IV. CALCULATION OF π-a_1 MIXING

For the study of pseudoscalar-axial-vector mixing we generalize Eq. (3.1) to read

$$T_\pi(P^2)=i\gamma_5 T^{PP}(P^2)i\gamma_5+i\gamma_5 T^{PA}_\mu(P^2)\gamma^\mu\gamma_5 + \gamma^\mu\gamma_5 T^{AP}_\mu(P^2)i\gamma_5+\gamma^\mu\gamma_5 T^{AA}_{\mu\nu}(P^2)\gamma^\nu\gamma_5. \tag{4.1}$$

We define

$$T^{PA}_\mu(P^2)=\frac{iP_\mu}{\sqrt{P^2}}T^{PA}(P^2), \tag{4.2}$$

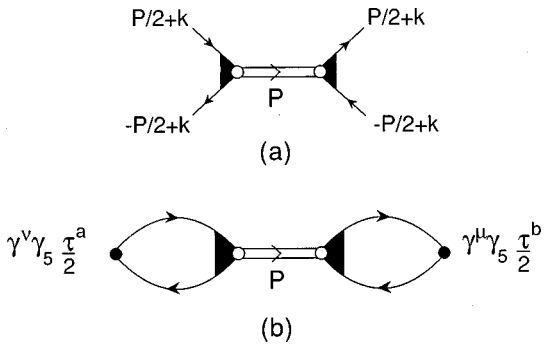

FIG. 7. (a) A T matrix, including the vertex of the confining interaction for the external lines, is shown. (b) A resonant contribution to a current correlator is obtained from the diagram in (a) by introducing currents that excite and deexcite the $q\overline{q}$ pairs. Here we consider the correlator of two axial-vector currents of the form $\overline{q}(x)\gamma^\mu\gamma_5(\tau^i/2)q(x)$.

$$T^{AP}_\mu(P^2)=\frac{iP_\mu}{\sqrt{P^2}}T^{AP}(P^2), \tag{4.3}$$

and

$$T^{AA}_{\mu\nu}(P^2)=\frac{P_\mu P_\nu}{P^2}T^{AA}_L(P^2). \tag{4.4}$$

We then consider the matrix

$$T(P^2)=\begin{pmatrix} T^{PP}(P^2) & iT^{PA}(P^2) \\ iT^{AP}(P^2) & T^{AA}_L(P^2)\end{pmatrix} \tag{4.5}$$

which acts in the space spanned by $i\gamma_5$ and $\gamma_0\gamma_5$ when $\vec{P}=0$, so that we write

$$\hat{T}=(i\gamma_5,\gamma^0\gamma_5)\begin{pmatrix} T^{PP}(P^2) & iT^{PA}(P^2) \\ iT^{AP}(P^2) & T^{AA}_L(P^2)\end{pmatrix}\begin{pmatrix} i\gamma_5 \\ \gamma^0\gamma_5\end{pmatrix}. \tag{4.6}$$

The various elements of this matrix are given in Ref. [2]. Rather than repeat that material here, we will present the results of our calculation.

In this case the $\hat{T}$ matrix may be brought to diagonal form by a matrix

$$M(\theta)=\begin{pmatrix}\cos\theta & i\sin\theta \\ i\sin\theta & \cos\theta\end{pmatrix}, \tag{4.7}$$

such that

$$M(\theta)T_\pi(P^2)M^{-1}(\theta)=\begin{pmatrix} T_1(P^2) & 0 \\ 0 & T_2(P^2)\end{pmatrix}. \tag{4.8}$$

If we assume there is a resonance in $T_1(P^2)$, we would have, when $\vec{P}=0$,

$$T_1(P^2)=i[\cos\theta\gamma_5+\sin\theta\gamma^0\gamma_5]\frac{g^2_{\pi' qq}}{P^2-m^2_{\pi'}} \times i[\cos\theta\gamma_5+\sin\theta\gamma^0\gamma_5], \tag{4.9}$$

so that for $\cos\theta=1$ we go over to Eq. (3.1). For a resonance in T_2, we have

$$T_2(P^2)=[-\sin\theta\gamma_5+\cos\theta\gamma^0\gamma_5]\frac{g^2_{\pi' qq}}{P^2-m^2_{\pi'}}\times[-\sin\theta\gamma_5+\cos\theta\gamma^0\gamma_5]. \quad (4.10)$$

Now we include confinement in the numerator of the T matrix (see Fig. 3). We define

$$F_\pi(P,k)=i\cos\theta\gamma_5[b_0(P,k)+\not{P}b_1(P,k)]+i\sin\theta\frac{\not{P}}{\sqrt{P^2}}\gamma_5[d_0(P,k)+\not{P}d_1(P,k)], \quad (4.11)$$

where $b_0(P,k)$ and $b_1(P,k)$ have been defined previously. Here $d_0(P,k)$ and $d_1(P,k)$ describe confinement for the axial-vector vertex (see the Appendix). Thus, Eq. (3.4) may be generalized to read

$$T_1^\pi(P,k',k)=F_\pi(-P,k')\frac{g^2_{\pi' qq}}{P^2-m^2_{\pi'}}F_\pi(P,k), \quad (4.12)$$

with a similar equation for $T_2^\pi(P,k',k)$ based upon the form of Eq. (4.10).

It is often useful to use the *same* form for the T matrix, when a resonance appears in either T_1 or T_2. That may be accomplished by adding 90° to the mixing angle when the resonance is in T_2, and then using Eq. (4.9) or Eq. (4.11) (see Tables I and II). From Table II, we see that the states of the π-a_1 system fall into two groups. There are three states with small mixing angles, which may be identified as the $\pi(1S)$, $\pi(2S)$, and $\pi(3S)$ states. The other states are strongly mixed and have similar angles.

V. VECTOR MESONS

We will discuss the ω and ϕ mesons and their radial excitations. In this case we have ideal mixing, which simplifies the discussion. It is useful to define a vacuum-polarization function for the up (and down) quark

$$-iJ_u^{\mu\nu}(P)=-n_c\int\frac{d^4k}{(2\pi)^4}\mathrm{Tr}\times[iS_u(P/2+k)\hat{\gamma}^\mu iS_u(-P/2+k)\hat{\gamma}^\nu], \quad (5.1)$$

where

$$\hat{\gamma}^\mu=\gamma^\mu-\frac{\not{P}P^\mu}{P^2}. \quad (5.2)$$

Here $S_u(k)=[\not{k}-m_u+i\epsilon]^{-1}$ is the propagator for the up quark. There is a similar definition of $J_s^{\mu\nu}(P)$ for the strange quark. With confinement, we define

$$-iJ_u^{\mu\nu}(P)=-n_c\int\frac{d^4k}{(2\pi)^4}\mathrm{Tr}\times[iS_u(P/2+k)\Gamma^\mu(P,k)iS(-P/2+k)\hat{\gamma}^\nu], \quad (5.3)$$

where $\Gamma^\mu(P,k)$ implements our confinement model.

We also put

$$J_u^{\mu\nu}(P)=-\hat{g}^{u\nu}(P)J_u^V(P^2), \quad (5.4)$$

$$J_s^{\mu\nu}(P)=-\hat{g}^{u\nu}(P)J_s^V(P^2), \quad (5.5)$$

$$J_\omega(P^2)=2J_u^V(P^2), \quad (5.6)$$

$$J_\phi(P^2)=2J_s^V(P^2), \quad (5.7)$$

and find the masses of the ω and ϕ mesons by solving

$$1-G_VJ_\omega(P^2)=0 \quad (5.8)$$

and

$$1-G_VJ_\phi(P^2)=0. \quad (5.9)$$

We also have

$$\frac{1}{g^2_{\omega qq}(m_\omega^2)}=\left.\frac{\partial J_\omega(P^2)}{\partial P^2}\right|_{P^2=m_\omega^2} \quad (5.10)$$

and

$$\frac{1}{g^2_{\phi qq}(m_\phi^2)}=\left.\frac{\partial J_\phi(P^2)}{\partial P^2}\right|_{P^2=m_\phi^2}, \quad (5.11)$$

for the ω and ϕ and their radial excitations.

In the absence of a confinement model we have, with $\bar{g}^{\mu\nu}(P)=g^{\mu\nu}-P^\mu P^\nu/P^2$

$$T_\omega(P)=-\frac{g^2_{\omega qq}(m_\omega^2)}{P^2-m_\omega^2+i\epsilon}\hat{\gamma}_\mu\bar{g}^{\mu\nu}(P)\hat{\gamma}_\nu, \quad (5.12)$$

while the introduction of confinement leads to

$$T_\omega(P,k',k)=-\frac{g^2_{\omega qq}(m_\omega^2)}{P^2-m_\omega^2}\Gamma^\mu(-P,k')\bar{g}_{\mu\nu}(P)\Gamma^\nu(P,k) \quad (5.13)$$

for each isolated resonance. Note that we need not write an $i\epsilon$ in the denominator of Eq. (5.13).

In general, $\Gamma^\mu(P,k)$ will contain eight terms. Our model, which makes use of Lorentz-vector confinement, and which has no energy transfer in the $\vec{P}=0$ frame yields a form of $\Gamma^\mu(P,k)$ that has only four terms [3]

TABLE III. Experimental values for the masses and decay constants [13] are compared to our theoretical values. Here $m_u = m_d = 0.364\,\mathrm{GeV}$, $m_s = 0.565\,\mathrm{GeV}$, $\kappa_V = 0.0575\,\mathrm{GeV}^2$, $\Lambda_3 = 0.622\,\mathrm{GeV}$, and $G_V = 12.50\,\mathrm{GeV}^{-2}$.

Meson	Mass (expt) (MeV)	Mass (theory) (MeV)	$g_{\omega qq}$ or $g_{\phi qq}$	Decay constant (f_ω, f_ϕ) (MeV) expt	theory
$\omega(782)$	781±0.12	782[a]	3.93	45.9±0.7	47.3
$\phi(1020)$	1019.413±0.008	1019[a]	4.78	78±2	62.5
$\omega(1420)$	1419±31	1402	1.26		8.4
$\omega(1600)$	1649±24	1650	0.861		4.9
$\phi(1680)$	1680±20	1717	0.731		5.8

[a]Fit by the choice of G_V and m_s.

$$\Gamma^\mu(P,k) = \frac{\hat{k}^\mu}{|\hat{k}^2|^{1/2}}\left[a_0(P,k) + \frac{\hat{\not{k}}}{|\hat{k}^2|^{1/2}} a_1(P,k) + \gamma^\mu_{\perp,k} a_2(P,k) + \frac{i\epsilon^{\mu\nu\rho\sigma}\gamma_5\gamma_\nu P_\rho \hat{k}_\sigma}{|P^2|^{1/2}|\hat{k}^2|^{1/2}} a_3(P,k)\right] \tag{5.14}$$

with

$$\gamma^\mu_{\perp,k} = \hat{\gamma}^\mu - \frac{\hat{\not{k}}\hat{k}^\mu}{\hat{k}^2} \tag{5.15}$$

and

$$\hat{k}^\mu(P) = k^\mu - \frac{(k\cdot P)P^\mu}{P^2}. \tag{5.16}$$

Procedures for obtaining the Lorentz-scalars a_0, a_1, a_2, and a_3 are described in Ref. [3]. We do not repeat that discussion here, since our goal is to exhibit the form of the T matrix and current correlators for our (covariant) model of confinement.

The ω and ϕ decay constants, f_ω and f_ϕ given by

$$\langle \mathrm{vac}|J^\mu_{em}|\omega,\lambda\rangle = m_\omega f_\omega \epsilon^\mu_\lambda(\vec{P}) \tag{5.17}$$

and

$$\langle \mathrm{vac}|J^\mu_{em}|\phi,\lambda\rangle = m_\phi f_\phi \epsilon^\mu_\lambda(\vec{P}). \tag{5.18}$$

Here $\epsilon^\mu_\lambda(\vec{P})$ is the polarization four vector for the ω or ϕ. We see that

$$f_\omega = \frac{g_{\omega qq}(m_\omega^2)}{\sqrt{2}} J^V_u(m_\omega^2)\left(\frac{2}{3} - \frac{1}{3}\right), \tag{5.19}$$

where the last factor arises from the charges of the up and down quarks. Also,

$$f_\phi = g_{\phi qq}(m_\phi^2) J^V_s(m_\phi^2)(\tfrac{1}{3}). \tag{5.20}$$

If we define a correlator

$$C^{\mu\nu}(P) = \int d^4x e^{iP\cdot x}\langle \mathrm{vac}|T[J^\mu_{em}(x)J^\nu_{em}(0)]|\mathrm{vac}\rangle, \tag{5.21}$$

$$= -\tilde{g}^{\mu\nu} C(P^2), \tag{5.22}$$

we can relate the contribution of each resonance to $C(P^2)$ to the T matrix of Eq. (5.13), using the relation

$$\tilde{g}^{\mu\nu}(P) = -\sum_{\lambda=1}^{3} \epsilon^\mu_\lambda(\vec{P})\epsilon^\nu_\lambda(\vec{P}) \tag{5.23}$$

and including the electromagnetic charge operator at each vertex (see Fig. 7).

Results of our study of the ω and ϕ mesons and their radial excitations are given in Table III. We have used $\Lambda_3 = 0.622\,\mathrm{GeV}$ as a momentum cutoff $|\vec{k}| \leq \Lambda_3$, in our calculation of the polarization integrals.

VI. SINGLET-OCTET MIXING FOR THE η AND η' MESONS

In this section we are interested in exhibiting the T matrix for the mixing of the SU(3) singlet η^0 with the (octet) η^8. We will then go on to discuss pseudoscalar-axial-vector mixing in addition to singlet-octet mixing in the next section. It is useful to write the T matrix in the form

$$\hat{T}_P(P^2) = \Phi^T T_P(P^2)\Phi \tag{6.1}$$

with

$$\Phi = \begin{pmatrix} \lambda_8 \\ \lambda_0 \end{pmatrix} \tag{6.2}$$

and

$$T_P(P^2) = \begin{pmatrix} A_P(P^2) & B_P(P^2) \\ B_P(P^2) & C_P(P^2) \end{pmatrix}. \tag{6.3}$$

The expressions for $A_P(P^2)$, $B_P(P^2)$, and $C_P(P^2)$ given in Ref. [2]. We then introduce a matrix $M(\theta)$, such that

TABLE IV. Mass spectrum and mixing angles for states of the η-η' system. For the first three columns $G_D=-200\ \mathrm{GeV}^{-5}$, $G_S=11.38\ \mathrm{GeV}^{-2}$, and only singlet-octet mixing is included. For the last column, pseudoscalar-axial-vector mixing is taken into account, G_D is reduced to $-64.0\ \mathrm{GeV}^{-5}$, and $G_S=12.2\ \mathrm{GeV}^{-2}$ is used. Here $m_u=0.364$ GeV and $m_s=0.565$ GeV. For a resonance in T_1 we have $\eta=\cos\theta_P\eta^8-\sin\theta_P\eta^0$, while for a resonance in T_2, we have $\eta'=\sin\theta_P\eta^8+\cos\theta_P\eta^0$.

Mass (theory) (GeV)	$\theta_P(P^2)$ (deg)	Channel	Fraction of $\bar{s}s$ configuration	Mass (GeV) $G_D=-64.0\ \mathrm{GeV}^{-5}$
0.512	−11.5	T_1	0.468[a]	0.531
0.977	−36.3	T_2	0.897[b]	0.972
1.37	−62.5	T_1	0.018[a]	1.36
1.64	41.5	T_2	0.012[b]	1.63
1.69	35.3	T_1	0.998[a]	1.69

[a]Calculated on the assumption that the resonance appears only in T_1.
[b]Calculated on the assumption that the resonance appears entirely in T_2.

$$\begin{pmatrix}\eta\\ \eta'\end{pmatrix}=M(\theta)\begin{pmatrix}\eta^8\\ \eta^0\end{pmatrix} \tag{6.4}$$

with

$$M(\theta)=\begin{pmatrix}\cos\theta & -\sin\theta\\ \sin\theta & \cos\theta\end{pmatrix}. \tag{6.5}$$

The matrix $M(\theta)$ brings $T_P(P^2)$ to diagonal form

$$M(\theta)T_P(P^2)M^{-1}(\theta)=\begin{pmatrix}T_1(P^2) & 0\\ 0 & T_2(P^2)\end{pmatrix}. \tag{6.6}$$

For example, for the η, which appears as a resonance in $T_1(P^2)$,

$$\tilde{T}_\eta(P,k',k)=\Gamma_\eta(P,k')i\gamma_5\frac{g^2_{\eta qq}}{P^2-m^2_\eta}i\gamma_5\Gamma_\eta(P,k), \tag{6.7}$$

with

$$\Gamma_\eta(P,k)=[b_0(P,k)+\not{P}b_1(P,k)][\cos\theta\lambda_8-\sin\theta\lambda_0]. \tag{6.8}$$

For the η', which appear as a resonance in $T_2(P^2)$, we have

$$\tilde{T}_{\eta'}(P,k',k)=\Gamma_{\eta'}(P,k')i\gamma_5\frac{g^2_{\eta' qq}}{P^2-m^2_{\eta'}}i\gamma_5\Gamma_{\eta'}(P,k), \tag{6.9}$$

with

$$\Gamma_{\eta'}(P,k)=[b_0(P,k)+\not{P}b_1(P,k)][\sin\theta\lambda_8+\cos\theta\lambda_0]. \tag{6.10}$$

Inclusion of the propagators for the external lines yields a Green's function

$$\begin{aligned}G_\eta(P,k',k)=&[S(P/2+k')\Gamma_\eta(P,k')i\gamma_5S(-P/2+k')]\\ &\times\frac{g^2_{\eta qq}}{P^2-m^2_\eta}\\ &\times[S(P/2+k)i\gamma_5\Gamma_\eta(P,k)S(-P/2+k)].\end{aligned} \tag{6.11}$$

Our results for a study of singlet-octet mixing are given in Table IV [2]. The value of $\theta=-11.5°$ for the $\eta(547)$ is typical for calculations of this type [12]. Mass values for the case that pseudoscalar-axial-vector coupling is considered, in addition to singlet-octet mixing, are given in the last column of Table IV. (A much smaller value of G_D is needed to fit the $\eta(547)$ and $\eta'(958)$ masses values in that case.)

VII. ROLE OF PSEUDOSCALAR-AXIAL-VECTOR MIXING FOR THE η AND η' MESONS

In this case the T matrix acts in the space with components $i\gamma_5\lambda_8$, $i\gamma_5\lambda_0$, $\gamma_0\gamma_5\lambda_8$, and $\gamma_0\gamma_5\lambda_0$. It is desirable to use some of the notation of Ref. [12] and consider the T matrix in the space of $i\gamma_5\lambda_8$, $i\gamma_5\lambda_0$, $i\gamma_0\gamma_5\lambda_8$, and $i\gamma_0\gamma_5\lambda_0$, so as to deal entirely with matrices with real matrix elements. The structure of the T matrix and the associated equations are given in the Appendix to Ref. [12] and we do not reproduce them here, since we are mainly interested in seeing how confinement modifies the structure of the T matrix.

For each state, we write the T matrix in the *same form* rather than use different forms, as in Eqs. (6.7) and (6.9). We now assume that the T matrix has been brought to diagonal form. In general, we may write for a resonant diagonal component of the T matrix

$$T_\eta(P^2)=\frac{\nu_\eta(-P)\nu_\eta(P)}{P^2-m^2_\eta} \tag{7.1}$$

with

$$\begin{aligned}\nu_\eta(P)=&g_\eta i\gamma_5(-\sin\hat{\theta}\lambda_0+\cos\hat{\theta}\lambda_8)\\ &+\frac{\tilde{g}_\eta}{2m_{us}}i\not{P}\gamma_5(-\sin\tilde{\theta}\lambda_0+\cos\tilde{\theta}\lambda_8).\end{aligned} \tag{7.2}$$

TABLE V. Values of the mixing angles and coupling constants for the vertex of Eq. (7.2) are shown. Here $G_D=-64.0\,\mathrm{GeV}^{-5}$, $G_S=12.2\,\mathrm{GeV}^{-2}$, $G_V=12.5\,\mathrm{GeV}^{-2}$, and $m_{us}=0.433\,\mathrm{GeV}$.

Mass (GeV)	$\hat{\theta}(P^2)$ (deg)	$\tilde{\theta}(P^2)$ (deg)	g_η	$\tilde{g}_\eta$
0.531	−36.7	−42.9	5.50	1.90
0.972	−135	−127	5.54	1.67
1.36	−59.6	160.3	1.19	0.074
1.63	−135.3	−121	0.380	0.365
1.69	−52.9	−56.4	0.500	0.460

It is this form that is used to parametrize the T matrix at each resonance, with the results given in Table V.

We may now define a T matrix with confinement vertices in the numerator (see Fig. 6). We write

$$T_\eta(P,k',k)=\frac{f_\eta(-P,k')f_\eta(P,k)}{P^2-m_\eta^2} \tag{7.3}$$

with

$$f_\eta(P,k)=g_\eta i\gamma_5[b_0(P,k)+\not{P}b_1(P,k)]\times(-\sin\hat{\theta}\lambda_0+\cos\hat{\theta}\lambda_8)+\frac{\tilde{g}_\eta}{2m_{us}}i\not{P}\gamma_5(d_0(P,k)+\not{P}d_1(P,k))(-\sin\tilde{\theta}\lambda_0+\cos\tilde{\theta}\lambda_8). \tag{7.4}$$

We have used $m_{us}=0.433\,\mathrm{GeV}$.

From our previous discussion and from the Appendix, we can see that, in the absence of confinement, $b_0(P,k)=1$, $b_1(P,k)=0$, $d_0(P,k)=1$, and $d_1(P,k)=0$, so that Eq. (7.3) will reduce to Eq. (7.1). Values for g_η, $\tilde{g}_\eta$, $\hat{\theta}(P^2)$, and $\tilde{\theta}(P^2)$ are given in Table V for a calculation with $G_D=-64.0\,\mathrm{GeV}^{-5}$. This is a quite small value of G_D and leads to what is essentially ideal mixing for the η and η'. Clearly the wave functions of the η and η' with four components are significantly more complicated than those usually considered. It remains to be seen whether the experimental values for the decays of the η and η' can be obtained with such wave functions.

VIII. DISCUSSION

Reference [12] contains a general discussion of T matrices for mesons (including singlet-octet and pseudoscalar-axial-vector mixing) in the absence of a confinement model. In our work, one of our goals has been to show how the results of Ref. [12] are modified in the presence of confining interaction. It is necessary to include such an interaction, if one wishes to describe mesons whose masses are greater than about 600 MeV. such as the ω, ρ, ϕ, and η' mesons. If we include confinement, we can also describe various radial excitations of the π, ω, ρ, ϕ and η mesons, among others (see Tables I–V).

Further work is needed in the case of the η-η' system. With the inclusion of pseudoscalar-axial-vector coupling, we saw we could fit the η and η' mass values with a very small value of the 't Hooft interaction. That leads to ideal mixing for η-η' states. This result may be tested by calculating the rates for $\eta\to2\gamma$ and $\eta'\to2\gamma$. In the presence of confinement, such calculations are rather complicated. We hope to report theoretical results for the η and η' decay rates in a future publication.

APPENDIX

In this appendix we summarize some results for the (longitudinal) axial-vector vertex. That vertex satisfies the equation

$$\overline{\Gamma}_L^\mu(P,k)=\frac{P^\mu\not{P}}{P^2}\gamma_5-i\int\frac{d^4k'}{(2\pi)^4}[\gamma^\rho S(P/2+k')\overline{\Gamma}_L^\mu(P,k')\times S(-P/2+k')\gamma_\rho V^c(\vec{k}-\vec{k}')]. \tag{A1}$$

It is useful to define Γ_L^{+-} and Γ_L^{-+}:

$$\Lambda^{(+)}(\vec{k})\overline{\Gamma}_L^\mu(P,k)\Lambda^{(-)}(-\vec{k})=\frac{P^\mu}{\sqrt{P^2}}\Gamma_L^{+-}(P,k)\Lambda^{(+)}\times(\vec{k})\gamma_5\Lambda^{(-)}(-\vec{k}) \tag{A2}$$

and

$$\Lambda^{(-)}(-\vec{k})\overline{\Gamma}_L^\mu(P,k)\Lambda^{(+)}(\vec{k})=\frac{P^\mu}{\sqrt{P^2}}\Gamma_L^{-+}(P,k)\times\Lambda^{(-)}(-\vec{k})\gamma_5\Lambda^{(+)}(\vec{k}). \tag{A3}$$

We have the equations

$$\Gamma_L^{+-}(P^0,|\vec{k}|)=\frac{m}{E(k)}+\int\frac{d^3k'}{(2\pi)^3}\frac{V^C(\vec{k}-\vec{k}')}{P^0-2E(\vec{k}')}\times\frac{2E(\vec{k})E(\vec{k}')-m^2}{E(\vec{k})E(\vec{k}')}\Gamma_L^{+-}(P^0,|\vec{k}'|) \tag{A4}$$

and

$$\Gamma_L^{-+}(P^0,|\vec{k}|)=-\frac{m}{E(k)}-\int\frac{d^3k'}{(2\pi)^3}\frac{V^C(\vec{k}-\vec{k}')}{P^0+2E(\vec{k}')}\times\frac{2E(\vec{k})E(\vec{k}')-m^2}{E(\vec{k})E(\vec{k}')}\Gamma_L^{-+}(P^0,|\vec{k}'|) \tag{A5}$$

that are used to calculate Γ_L^{+-} and Γ_L^{-+}.

We now introduce the scalar invariants d_0 and d_1 by the relation

$$\overline{\Gamma}_L(P,k)=\frac{\not{P}}{\sqrt{P^2}}\gamma_5[d_0(\sqrt{P^2},\sqrt{-k_c^2})+\not{P}d_1(\sqrt{P^2},\sqrt{-k_c^2})]. \tag{A6}$$

If $\vec{P}=0$, the last equation reads

$$\bar{\Gamma}_L(P^0,|\vec{k}|)=\gamma_0\gamma_5[d_0(P^0,|\vec{k}|)+\gamma_0 P^0 d_1(P^0,|\vec{k}|)]. \tag{A7}$$

Therefore, we find

$$\Gamma_L^{+-}(P^0.|\vec{k}|)=\frac{m}{E(\vec{k})}d_0(P^0,|\vec{k}|)-P^0 d_1(P^0,|\vec{k}|) \tag{A8}$$

and

$$\Gamma_L^{-+}(P^0,|\vec{k}|)=-\frac{m}{E(\vec{k})}d_0(P^0,|\vec{k}|)-P^0 d_1(P^0,|\vec{k}|). \tag{A9}$$

Thus

$$d_0(P^0,|\vec{k}|)=\frac{E(\vec{k})}{2m}[\Gamma_L^{+-}(P^0,|\vec{k}|)-\Gamma_L^{-+}(P^0,|\vec{k}|)] \tag{A10}$$

and

$$d_1(P^0,|\vec{k}|)=-\frac{1}{2P^0}[\Gamma_L^{+-}(P^0,|\vec{k}|)+\Gamma_L^{-+}(P^0,|\vec{k}|)]. \tag{A11}$$

[1] For reviews of the NJL model see, T. Hadsuda and T. Kunihoro, Phys. Rep. **247**, 221 (1994); U. Vogl and W. Weise, Prog. Part. Nucl. Phys. **27**, 195 (1991); S. P. Klevansky, Rev. Mod. Phys. **64**, 649 (1992); G. Ripka, *Quarks Bound by Chiral Fields* (Oxford University Press, Oxford, 1997).

[2] Bo Huang, Xiang-Dong Li, and C. M. Shakin, Phys. Rev. C **58**, 3648 (1998).

[3] L. S. Celenza, Bo Huang, and C. M. Shakin, Phys. Rev. C **59**, 1041 (1999), following paper. Report No. BCCNT 97/071/271, 1998.

[4] L. S. Celenza, Xiang-Dong Li, and C. M. Shakin, Phys. Rev. C **56**, 3326 (1997).

[5] L. S. Celenza, Xiang-Dong Li, and C. M. Shakin, Phys. Rev. C **55**, 1492 (1997).

[6] L. S. Celenza, C. M. Shakin, Wei-Dong Sun, J. Szweda, and Xiquan Zhu, Phys. Rev. D **51**, 3638 (1995).

[7] J. Praschifka, C. D. Roberts, and R. T. Cahill, Phys. Rev. D **36**, 209 (1987).

[8] R. D. Roberts, R. T. Cahill, and J. Praschifka, Ann. Phys. (N.Y.) **188**, 20 (1988).

[9] P. C. Tandy, Prog. Part. Nucl. Phys. **39**, 117 (1994).

[10] H. J. Munczek and P. Jain, Phys. Rev. D **46**, 438 (1992).

[11] P. Jain and H. J. Munczek, Phys. Rev. D **48**, 5403 (1993).

[12] S. Klimt, M. Lutz, U. Vogl, and W. Weise, Nucl. Phys. **A516**, 429 (1990).

[13] Particle Data Group, R. M. Barnett *et al.*, Phys. Rev. D **54**, 1 (1996).